Journal of Materials Chemistry A

PAPER

View Article Online
View Journal | View Issue

Cite this: J. Mater. Chem. A, 2014, 2, 17925

A high voltage solar cell using a donor–acceptor conjugated polymer based on pyrrolo[3,4-*f*]-2,1,3-benzothiadiazole-5,7-dione†

Hairong Li,‡[ab] Shuangyong Sun,‡[a] Subodh Mhaisalkar,[ab] Melvin T. Zin,§[c] Yeng Ming Lam*[ab] and Andrew C. Grimsdale*[ab]

Received 13th March 2014
Accepted 5th September 2014

DOI: 10.1039/c4ta01248h

www.rsc.org/MaterialsA

We report an improved synthesis of the electron-accepting unit pyrrolo[3,4-*f*]-2,1,3-benzothiadiazole-5,7-dione (BTI) and the synthesis and characterisation of two donor–acceptor copolymers containing it: poly[6-dodecyl-4,8-bis(2-thienyl)pyrrolo[3,4-*f*]-2,1,3-benzothiadiazole-5,7-dione-*alt*-9,9-dioctyl-2,7-bis(thien-2′-yl)-9*H*-fluorene] (P(BTI-F)), and poly[6-dodecyl-4,8-bis(thien-2′-yl)pyrrolo[3,4-*f*]-2,1,3-benzothiadiazole-5,7-dione-*alt*-4,8-bis(octyloxy)benzo[1,2-*b*:4,5-*b*′]dithiophene] (P(BTI-B)). By the incorporation of an imide group onto a benzothiadiazole moiety, the HOMO level is lowered. To explore the effectiveness of conjugation along the polymer backbone, two electron donors: fluorene and benzobithiophene, were introduced. These represent a weak and a strong electron-donor, respectively. Both polymers have low lying HOMOs and hence are thermally stable and also result in high open-circuit voltages (V_{oc}) in photovoltaic applications. Compared to P(BTI-B), P(BTI-F) has a larger bandgap due to the incorporation of a weaker donor unit and thus a deeper lying HOMO level. Devices based on P(BTI-F) and [6,6]-phenyl-C_{61}-butyric acid methyl ester ($PC_{61}BM$) can obtain a remarkably high V_{oc} of 1.11 V, but a PCE of only 1.61%. By contrast, polymer P(BTI-B) has stronger absorption in the longer wavelength range and can achieve a well-dispersed nanomorphology with $PC_{61}BM$ for efficient exciton dissociation, achieving PCE of 3.42%, with a J_{sc} of 9.71 mA cm^{-2}, V_{oc} of 0.75, and FF of 0.47.

Introduction

Benzo[*c*][2,1,3]thiadiazole (BT)[1–34] and its derivatives such as benzo[1,2-*c*:4,5-*c*′]bis[1,2,5]thiadiazole (BBT),[35–46] [1,2,5]-thiadiazolo[3,4-*g*]quinoxaline (TQ)[2,47–62] represent one of the most widely studied class of electron-accepting units for making donor–acceptor (D–A) polymers or small molecules. Attributed to the tunable electronic structures (HOMO, LUMO, bandgap), versatile chemical functionalization and robust properties, their electronic device applications such as organic field-effect transistors (OFET), organic light-emitting diodes (OLED), organic photovoltaics (OPV) and electrochromic devices have been extensively explored. An important structural feature of many BT-type materials is the attachment of the two flanking thienyl units at the 4,7-positions of BT, which results in large electron delocalization along the thiophene–benezene–thiophene direction due to strong quinoid character of the BT unit and reduced steric hindrance, thereby reducing the band gap and facilitating the intermolecular π–π interactions and charge transport.[44,61,63] However, one of the main disadvantages of BT based monomers is their poor solubility and they must be coupled with donor monomers that contain sufficiently long alkyl chain to make the polymer soluble. In earlier work we increased the solubility of such polymers by attaching alkoxy chains on the 5,6-positions of BT but this resulted in strong electron localization effect within BT and hence the bandgap remained at ~2 eV even when very electron-donating units such as benzo[1,2-*b*:4,5-*b*′]dithiophene (BDT), dithieno[3,2-*b*:2′,3′-*d*]silole and thieno[3,2-*b*]thiophene were coupled to these BT polymers.[6] To address this issue we herein report the synthesis of halogenated pyrrolo[3,4-*f*]-2,1,3-benzothiadiazole-5,7-dione (BTI) units enabling their more easy incorporation into polymers or oligomers. The introduction of the imide group onto BT not only facilitates the alkylation but also lowers the HOMO level to possibly obtain a high solar cell open circuit voltage V_{oc} while maintaining a reduced band gap. Fluorene and benzobithiophene representing a weak and a strong electron-donor,

[a]School of Materials Science and Engineering, Nanyang Technological University, Block N4.1, 50 Nanyang Avenue, 639798, Singapore. E-mail: ymlam@ntu.edu.sg; acgrimsdale@ntu.edu.sg

[b]Energy Research Institute @ NTU (ERI@N), Nanyang Technological University, 50 Nanyang Drive, 637533, Singapore

[c]3M Research Centre, 100 Woodlands Avenue 7, 738205, Singapore

† Electronic supplementary information (ESI) available: Single crystal XRD data file of the compound **5**, named "BTI_XRD.cif". CCDC 965762. For ESI and crystallographic data in CIF or other electronic format see DOI: 10.1039/c4ta01248h

‡ These authors contributed equally to this work.

§ Current address: 3M Electronics Markets Materials Division, 222 Tianlin Road, Shanghai 200233.

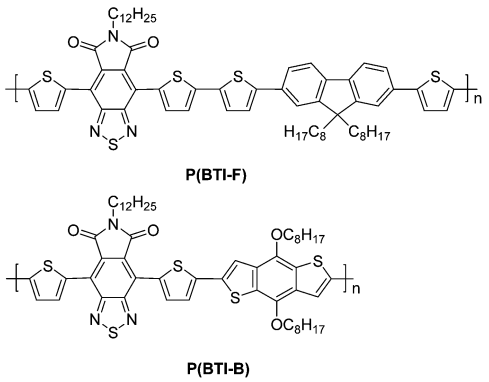

Fig. 1 Chemical structures of the two BTI based polymers.

respectively, were introduced to explore the effectiveness of conjugation along the polymer backbonein two D–A conjugated polymers, P(BTI-F) and P(BTI-B), shown in Fig. 1. The promising device performance using blends of these copolymers with fullerene acceptors in bulk heterojunction (BHJ) solar cells are also reported, in comparison to the performance reported for other polymers containing BTI units.

Experimental section

Materials and equipments

Chemicals and reagents were purchased from either Aldrich or Alfa-Aesar and were used without further purification unless otherwise stated. Tetrahydrofuran (THF) was freshly distilled over sodium wire before use. *N*-Bromosuccinimide (NBS) was recrystallised from distilled water before use. Column chromatography was carried out with Merck silica-gel (230–400 mesh) while thin layer chromatography (TLC) were performed on Merck silica-gel 60 PEG-backed plates (20 cm × 20 cm). The NMR spectra were collected on a Bruker DPX 400 spectrometer using chloroform-d as solvent and tetramethylsilane (TMS) as internal standard. Matrix assisted laser desorption/ionization time-of-flight (MALDI-TOF) mass spectra were obtained on a Shimadzu AXIMA Performance. Elemental analysis was obtained *via* a Thermo Scientific Flash 2000 Series CHNS Analyzer. Thermogravimetric analysis (TGA) was carried out using a TA Instrument Q500 Thermogravimetric Analyzer at a heating rate of 10 °C min^{-1} up to 900 °C and at a nitrogen flow rate of 75 cm^3 min^{-1}. Differential scanning calorimetry (DSC) was run on a TA Instrument Q10. Molecular weight of polymers was determined by gel permeation chromatography (GPC) method in chloroform, which was performed on Agilent GPC 1100 series model G1311A. In this method, column of PL gel 5 μm, MIXED-C was used and polystyrene was used as a standard, THF was used as the eluent at 20 °C with flow rate of 1 mL min^{-1}. UV-Vis absorption spectra were recorded on a Shimadzu UV-Vis 2501 spectrometer. Cyclic Voltammograms (CV) of the polymers were recorded on a CHI 660 electrochemical workstation in an acetonitrile solution of tetrabutylammoniun hexafluorophosphate (Bu_4NPF_6) (0.1 M) at scanning rate of 100 mV s^{-1}. The experiments were carried out at room temperature with a conventional three electrode configuration consisting of a platinum working electrode coated with polymer film, a gold counter electrode, and aSCE (saturated calomel electrode) reference electrode (−4.40 eV relative to vacuum calibrated by Fc/Fc^+).[64] The HOMO, LUMO energy levels and electrochemical band gaps were calculated by the following equations:

$$\text{HOMO} = -(4.40 + \text{oxidation onset}) \text{ eV} \quad (1)$$

$$\text{LUMO} = -(4.40 + \text{reduction onset}) \text{ eV} \quad (2)$$

$$E_g = \text{LUMO} - \text{HOMO} \quad (3)$$

Single X-ray diffraction data were collected on a Bruker AXS SMART CCD 3-circle diffractometer with a Mo-Kα radiation (0.71073 Å). The software used was SMART22 for collecting frames of data, indexing reflections, and determining lattice parameters; SAINT22 for integration of the intensity of reflections and scaling; SADABS23 for absorption correction; and SHELXTL24 for space group determination, structure solution, and least-squares refinements on F2. Structures were solved by direct methods and non-hydrogen atoms were refined anisotropically. Hydrogen atoms were introduced at fixed distances from carbon atoms and assigned fixed thermal parameters. All calculations were performed on a Silicon Graphics workstation, using programs provided by Siemens Pvt. Ltd.

Solar cells fabrication and characterization

The active films for the solar cells are made up of polymer:[6,6]-phenyl-C_{61}-butyric-acid methyl ester ($P_{61}CBM$) blended at different weight ratios (1 : 1, 1 : 2 and 1 : 3). Indium tin oxide (ITO)/glass substrates were purchased from Kintec Company (7 Ω sq^{-1}). The ITO/glass substrates were ultrasonic-cleaned by detergent, deionizer water, acetone and isopropanol for 15 min each in sequence. Following that, the ITO substrates were exposed for 2 min to air plasma. A layer of 30 nm of poly(3,4-ethylenedioxythiophene)-poly(styrenesulfonate) (PEDOT-PSS) film was spin-coated on ITO and then the substrates were baked at 140 °C for 10 min in a glove box. The polymer: $P_{61}CBM$ blend solutions were then spin-coated onto the PEDOT:PSS layer. The film thickness of the active layers is around 70 nm. For some devices, TiO_x ethanol solution was spin-coated on the photoactive layer to form electron buffer layer and hydrolysed in the ambient for 40 min. Finally, aluminium was deposited on the active layer under vacuum (10^{-6} torr) to form the cathode (~100 nm). The active area for each device was 0.07 cm^2. Current density–voltage (*J*–*V*) characteristics of the devices were measured using Agilent 4155C Semiconductor Parameter Analyzer under simulated AM 1.5G illumination (100 mW cm^{-2}). The external quantum efficiency (EQE) measurement was performed using the Merlin radiometer (Newport) with calibrated Si photodiode (Hamamatsu) as the reference. Atomic force microscopy (AFM) images were obtained on the Digital Instruments Nanoscope IIIausing the tapping mode.

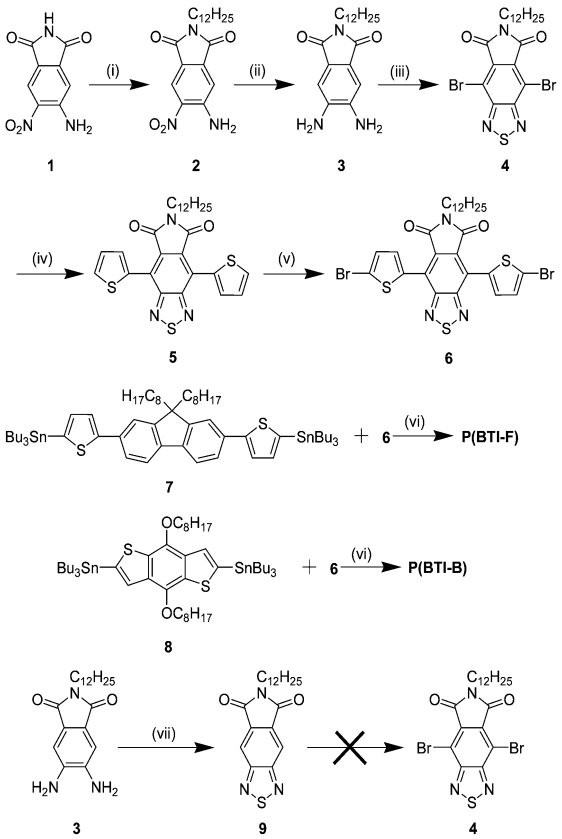

Scheme 1 Synthetic routes to the two polymers. Reaction conditions: (i) KOH, $C_{12}H_{25}Br$, EtOH, reflux. (ii) $SnCl_2$, HCl (37%), EtOH, reflux. (iii) Br_2, $SOCl_2$, $CHCl_3$, NEt_3, 0 °C to r.t. (iv) 2-ThSnBu_3, $PdCl_2(PPh_3)_2$, THF, reflux. (v) DMF, NBS, r.t. (vi) $PdCl_2(PPh_3)_2$, THF, reflux. (vii) $SOCl_2$, $CHCl_3$, pyridine, 0 °C to reflux.

Synthesis

The synthetic route is summarized in Scheme 1. 5-Amino-6-nitroisoindoline-1,3-dione (**1**)[65] and 2,7-bis(5-(tributylstannyl) thiophen-2-yl)-9,9′-bisoctyl-9*H*-fluorene (**7**)[66] and 4,8-bis(octyloxy)-2,6-bis(tributylstannyl)benzo[1,2-*b*;3,4-*b*′]dithiophene (**8**)[28] were synthesized according to literature procedures.

5-Amino-2-dodecyl-6-nitroisoindoline-1,3-dione (2). Compound **1** (10 g, 48.3 mmol), KOH (2.71, 17.0 g, 48.3 mmol) and $C_{12}H_{25}Br$ (12.0 g, 48.3 mmol) was dissolved in EtOH (70 mL). The solution was heated up to reflux for 1 day, cooled down and poured into water, and extracted with dichloromethane (DCM). The extract was washed with water, dried over anhydrous $MgSO_4$ and filtered. The filtrate was evaporated and the residue was purified by chromatography on silica eluting with dichloromethane (DCM) to yield (**2**) as a yelow solid (14.5 g, 85%). ^{1}H NMR ($CDCl_3$) δ: 8.62 (s, 1H, Ph*H*), 7.28 (s, 1H, Ph*H*), 6.76 (br, 2H, NH_2), 3.66 (t, $J = 7.2$ Hz, 2H, NCH_2), 1.65 (quintet, $J = 7.6$ Hz, 2H, NCH$_2$CH_2), 1.24–1.31 (m, 18H, CH_2), 0.87 (t, $J = 6.8$ Hz, 3H, CH_3). ^{13}C NMR ($CDCl_3$) δ: 167.18, 167.11, 149.5, 138.3, 134.5, 123.7, 119.5, 114.6, 39.3, 32.6, 30.3, 30.2, 30.1, 30.0, 29.8, 29.1, 27.5, 23.3, 14.8. MS (MALDI-TOF) *m*/*z*: 375.20 (M^+). Calcd *m*/*z* (100%): 375.22. Anal. calcd for $C_{20}H_{29}N_3O_4$: C, 63.98; H, 7.79; N, 11.19%. Found: C, 64.20; H, 7.67; N, 11.37%.

5,6-Diamino-2-dodecylisoindoline-1,3-dione (3). Compound **2** (5 g, 13.3 mmol) and $SnCl_2$ (5.1 g, 26.6 mmol) were dissolved in the solvent mixture of EtOH (100 mL) and 37% HCl (40 mL), the reaction mixture was brought to reflux for 6 h. Cooled down and precipitated from water, the white solid was washed thoroughly with water, MeOH and dried. The product was used immediately without further purification due to its instability in solution, though it was stable in the solid state as the 2HCl salt.

6-Dodecyl-4,8-dibromopyrrolo[3,4-*f*]-2,1,3-benzothiadiazole-5,7-dione (4). At 0 °C, $SOCl_2$ (2.2 g, 18.6 mmol) was added to the 100 mL $CHCl_3$ solution of compound **3** (1.6 g, 4.64 mmol) followed by addition of Br_2 (2.9 g, 18.6 mmol), the solution was stirred for 0.5 h in ice-water bath, then warmed up to r.t. and followed by addition of NEt_3 (4.7 g, 46.4 mmol), after overnight the solution was poured into water, extracted with DCM. The extract was washed with water, dried over anhydrous $MgSO_4$ and filtered. The filtrate was evaporated and the residue was purified by chromatography on silica eluting with DCM to yield (**4**) as white crystals (1.48 g, 60%). ^{1}H NMR ($CDCl_3$) δ: 3.77 (t, $J = 7.2$ Hz, 2H, NCH_2), 1.73 (quintet, $J = 7.6$ Hz, 2H, NCH$_2$CH_2), 1.24–1.35 (m, 18H, CH_2), 0.86 (t, $J = 6.8$ Hz, 3H, CH_3). ^{13}C NMR ($CDCl_3$) δ: 164.5, 156.0, 130.6, 113.6, 40.0, 32.5, 30.29, 32.23, 30.1, 30.0, 29.8, 28.8, 27.5, 23.3, 14.7. MS (MALDI-TOF) *m*/*z*: 530.92 (M^+). Calcd *m*/*z* (100%): 531.00. Anal. calcd for $C_{20}H_{25}Br_2N_3O_2S$: C, 45.21; H, 4.74; N, 7.91; S, 6.04%. Found: C, 45.37; H, 4.70; N, 8.13; S, 5.91%.

6-Dodecyl-4,8-di(thien-2′-yl)pyrrolo[3,4-*f*]-2,1,3-benzothiadiazole-5,7-dione (5). 1.2 g of compound **4** (2.26 mmol), 2.1 g of 2-tributylstannylthiophene (5.65 mmol) and 95 mg of Pd $[PPh_3]_2Cl_2$ (6 mol%) were added to a 100 mL round bottom flask purged with N_2 gas, followed by addition of 50 mL of fleshly distilled THF. The reaction was stirred under reflux for 1 day. The cooled mixture was poured into water and extracted with DCM. The organic layer was collected, dried over anhydrous $MgSO_4$ and concentrated. The filtrate was evaporated and the residue was purified by chromatography on silica eluting with DCM to yield (**5**) as yellow crystals (1.1 g, 90% yield). ^{1}H NMR ($CDCl_3$, δ ppm): 7.90 (dd, $J = 4$ Hz, 2H, Th*H*), 7.71 (dd, $J = 4.8$ Hz, 2H, Th*H*), 7.28 (m, 2H, Th*H*), 3.72 (t, $J = 7.6$ Hz, 2H, NCH_2), 1.69 (quintet, $J = 7.2$ Hz, 2H, NCH$_2$CH_2), 1.23–1.32 (m, 18H, CH_2), 0.87 (t, $J = 6.8$ Hz, 3H, CH_3). ^{13}C NMR ($CDCl_3$) δ: 166.43, 157.2, 133.7, 132.2, 130.8, 127.7, 127.5, 127.3, 39.6, 32.5, 30.28, 30.22, 30.1, 30.0, 29.8, 28.9, 27.6, 23.3, 14.7. MS (MALDI-TOF) *m*/*z*: 537.13 (M^+). Calcd *m*/*z* (100%): 537.16. Anal. calcd for $C_{28}H_{31}N_3O_2S_3$: C, 62.54; H, 5.81; N, 7.81; S, 17.89%. Found: 62.66; H, 5.74; N, 7.95; S, 17.76%.

6-Dodecyl-4,8-bis(5′-bromothiophen-2′-yl)pyrrolo[3,4-*f*]-2,1,-3-benzothiadiazole-5,7-dione (6). Compound **5** (1 g, 1.86 mmol) and NBS (0.73 g, 4.10 mmol) were dissolved in 40 mL DMF and stirred at r.t. overnight, the solution was poured into water and filtered, the solid was thoroughly washed with water and MeOH, then dried to yield (**6**) as an orange red solid in quantitative yield. ^{1}H NMR ($CDCl_3$, δ ppm): 7.78 (d, $J = 4$ Hz, 2H, Th*H*), 7.22 (d, $J = 4$ Hz, 2H, Th*H*), 3.73 (t, $J = 7.6$ Hz, 2H, NCH_2), 1.69 (quintet, $J = 7.2$ Hz, 2H, NCH$_2$CH_2), 1.23–1.33 (m, 18H, CH_2), 0.87 (t, $J = 6.8$ Hz, 3H, CH_3). ^{13}C NMR ($CDCl_3$) δ: 166.3, 156.6,

134.7, 133.7, 130.5, 127.1, 126.6, 119.3, 39.7, 32.5, 30.29, 30.23, 30.1, 30.0, 29.8, 28.9, 27.6, 23.3, 14.7. MS (MALDI-TOF) *m*/*z*: 694.91 (M^+). Calcd *m*/*z* (100%): 694.98. Anal. calcd for $C_{28}H_{29}Br_2N_3O_2S_3$: C, 48.35; H, 4.20; N, 6.04; S, 13.83%. Found: 48.56; H, 4.15; N, 6.21; S, 13.90%.

6-Dodecyl-pyrrolo[3,4-*f*]-2,1,3-benzothiadiazole-5,7-dione (9). At 0 °C, $SOCl_2$ (2.2 g, 18.6 mmol) was added to the 100 mL $CHCl_3$ solution of compound **3** (1.6 g, 4.64 mmol) followed by slow addition of anhydrous pyridine (3.7 g, 46.4 mmol) over 20 min, the solution was then brought to reflux stirred for 4 h. The solution was cooled down, poured into water and extracted with DCM. The extract was washed with water, dried over anhydrous $MgSO_4$ and filtered. The filtrate was evaporated and the residue was purified by chromatography on silica eluting with DCM to yield (**9**) as white crystals (1.48 g, 78%). ^{1}H NMR ($CDCl_3$) δ: 8.49 (s, 2H, Ph*H*), 3.77 (t, $J = 7.2$ Hz, 2H, NCH_2), 1.73 (quintet, $J = 7.6$ Hz, 2H, NCH$_2$CH_2), 1.24–1.34 (m, 18H, CH_2), 0.87 (t, $J = 6.8$ Hz, 3H, CH_3). ^{13}C NMR ($CDCl_3$) δ: 167.2, 157.4, 132.3, 118.8, 39.6, 32.6, 30.3, 30.2, 30.1, 30.0, 29.8, 29.0, 27.6, 23.3, 14.8. MS (MALDI-TOF) *m*/*z*: 373.09 (M^+). Calcd *m*/*z* (100%): 373.18. Anal. calcd for $C_{20}H_{27}N_3O_2S$: C, 64.31; H, 7.29; N, 11.25; S, 8.58%. Found: C, 64.57; H, 7.22; N, 11.34; S, 8.31%.

P(BTI-F). Compound **6** (0.45 g, 0.753 mmol), **7** (0.85 g, 0.753 mmol) and Pd[PPh_3]$_2Cl_2$ (30 mg, 6 mol%) were added to a 50 mL round bottom flask purged with N_2 gas, followed by addition of 20 mL of fleshly distilled THF. The reaction was stirred under reflux for 2 days, then cooled down and poured into methanol and filtered. The resulting solid was further purified by Soxhlet extraction using methanol, hexane and acetone to remove low MW polymers and impurities. Finally the polymers was extracted out using chloroform, which was evaporated under reduced pressure to afford the polymer as a black solid (0.48 g, 62%). ^{1}H NMR ($CDCl_3$) δ: 8.05 (br, Ar*H*), 7.88 (br, Ar*H*), 7.68 (br, Ar*H*), 7.59 (br, Ar*H*), 7.38 (br, Ar*H*), 3.74 (br, NCH_2), 2.05 (br, 9-CH_2 on fluorene), 1.72 (br, NCH$_2$CH_2), 1.10–1.35 (m, br, CH_2), 0.87 (br, CH_3), 0.80 (br, CH_3). Anal. calcd for $(C_{65}H_{73}N_3O_2S_5)_n$: C, 71.71; H, 6.76; N, 3.86; S, 14.73%. Found: C, 71.19; H, 7.02; N, 4.08; S, 14.27%. GPC: $M_n = 11\,263$ g mol^{-1}, $M_w = 21\,560$ g mol^{-1}, PDI = 1.91.

P(BTI-B). **P(BTI-B)** was synthesized by copolymerization of compound **6** and **8** by the same method as for polymer **P(BTI-F)**, as a black solid in 45% yield. ^{1}H NMR ($CDCl_3$) δ: 8.05 (br, Ar*H*), 7.76 (br, Ar*H*), 7.64 (br, Ar*H*), 7.38 (br, Ar*H*), 4.31 (br, OCH_2), 3.71 (br, NCH_2), 1.94 (br, OCH$_2$CH_2), 1.62 (br, NCH$_2$CH_2), 1.25–1.34 (m, br, CH_2), 0.90 (br, CH_3). Anal. calcd for $(C_{54}H_{65}N_3O_4S_5)_n$: C, 66.15; H, 6.68; N, 4.29; S, 16.35%. Found: C, 66.44; H, 6.89; N, 3.80; S, 15.85%. GPC: $M_n = 11\,454$ g mol^{-1}, $M_w = 17\,934$ g mol^{-1}, PDI = 1.57.

Results and discussion

Synthesis and characterization

All polymers were fully characterized and are readily soluble in chloroform, THF, chlorobenzene and 1,2-dichlorobenzene. The most critical synthetic intermediate is *N*-dodecyl-5,6-dicarboxylic imide-4,7-dibromo-benzo[*c*][2,1,3]thiadiazole (**4**). This compound was previously reported by us but without describing the synthetic details.[67] The synthesis which we now report here has considerable advantages over previous reports of BTI derivatives. The brominated dithienyl compound **6** has previously been made, and used to make some reduced bandgap polymers, including an analogue of P(BTI-B) bearing a branched alkyl chain on the BTI unit, by a totally different and less efficient synthetic route involving synthesis of the BTI unit from a different heterocycle.[68] Our route is shorter, more efficient and more flexible as it provides access to a wider range of polymers and oligomers. Compound *N*-dodecyl-5,6-dicarboxylic imide-benzo[*c*][2,1,3]-thiadiazole (**9**), has also previously been made by Chi *et al.* by a different method,[69] however all attempts to brominate the 4,7-positions of compound **9** including using bromine in strong acid at high temperature, were unsuccessful because of the deactivating imide and BT segments. Adding bromine to the reaction mixture of compound **3** before adding $SOCl_2$, also failed to produce **4** as the brominated diamine is too unstable to survive the annulation to form BT. Therefore, we controlled the reaction conditions so that Br_2 was added after formation of a ring structure but before the final dehydration to form BT stimulated by base. Our TLC results showed that as long as the time and temperature were properly controlled, the major product was compound **4** with a little mono-brominated side product and a negligible amount of compound **9**, both which could be removed by chromatography on silica.

The TGA and DSC results were shown in Fig. 2 and summarized in Table 1. Both polymers showed very high thermal stability. Decomposition (T_d in Table 1) of P(BTI-F) starts at 400 °C, while for P(BTI-B) it commences at 310 °C. It is obvious that the thermal stability is largely determined by the donor part wherein the bisthienylfluorene (F) is much more

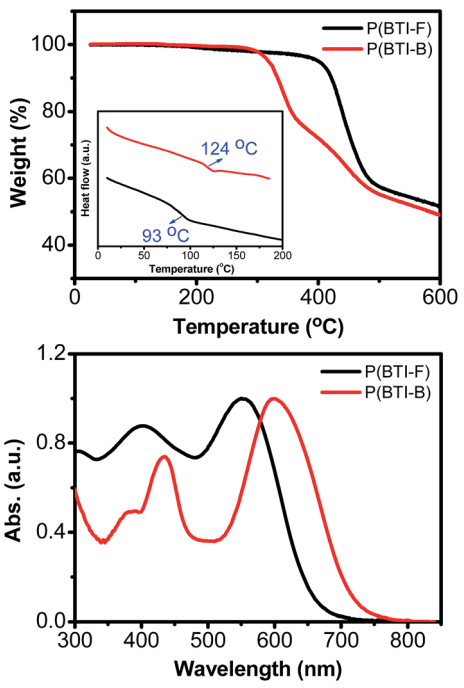

Fig. 2 Top: TGA and DSC (inset) of the two polymers; bottom: normalized absorption spectra of the two polymers in chloroform.

Table 1 Thermal, optical and electrochemical properties of the polymers

Polymers	P(BTI-F)	P(BTI-B)
HOMO (eV)	−5.60	−5.36
LUMO (eV)	−3.74	−3.68
E_g (eV)	1.86	1.68
λ_{max} (nm)	551, 403	610, 444, 392
T_d (°C)	400	310
T_g (°C)	93	124

stable than benzodithiophene (B). On the other hand, P(BTI-F) has a lowerglass transition temperature (T_g in Table 1) than P(BTI-B). Considering the same acceptor unit is in both polymers, the sp^3 configuration of the fluorene C9 bearing the alkyl chains in P(BTI-F) simply creates greater separation between the polymer chains during packing as compared to the planar benzodithiophene in P(BTI-B), resulting in higher flexibility at elevated temperatures.

The absorption spectra of the polymers were recorded in chloroform solution as shown in Fig. 2. The peak maxima (λ_{max}) and electrochemical band gaps (E_g) are summarized in Table 1. Comparing P(BTI-F) with P(BTI-B), the peak maximum attributed to the π–π* absorption of the conjugated polymer backbone for the former (560 nm) is 50 nm shorter than the latter (610 nm), which implies the benzodithiophene in P(BTI-B) increases the intramolecular charge transfer (ICT) between donor and acceptor, causing more electronic delocalization along the polymer backbones.[70] The electron rich BDT unit has been widely incorporated into D–A polymer structures, leading to a range of the bandgaps even down to 1 eV when coupling with a variety of acceptors,[28,29,71–75] it is not surprising to observe that the stronger donor–acceptor interaction in P(BTI-B) significantly lower the band gap as compared to the weaker donor in P(BTI-F) (E_g in Table 1). Cyclic voltammetry measurements (Fig. 3) revealed that both polymers had close lowest unoccupied molecular orbital (LUMO) energy levels, which can be attributed to the dominating effect of the electron-withdrawing BTI unit. When comparing P(BTI-F) with P(BTI-B), the stronger donor in the latter raises the level of the highest occupied molecular orbital (HOMO) significantly (Table 1).

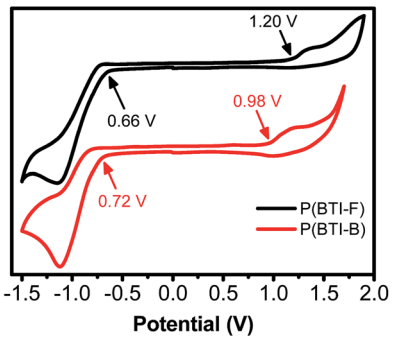

Fig. 3 CV spectra of the polymers.

A single crystal X-ray diffraction study of compound **5** revealed that the central BTI core was almost planar while the thiophene groups at 4,7-positions were twisted from the central core (Fig. 4). The sulfur atoms on both thiophene groups pointed towards the same direction relative to the plane of the central core and oriented closer to the thiadiazole side. It was interesting to observe that this molecule packed as a pair with both molecules oriented in the same direction, *i.e.* alkyl chain to alkyl chain, core to core. The measurement of torsion angle between two thiophenes and the connected central benzene also confirmed that there were four different values: 40.84°, 44.10° for one and 39.87°, 41.83° for the other, which also indicated that both thiophene groups at 4,7-positions in this molecule were not completely mirror symmetrical.

Solar cell performance

The photovoltaic properties of both polymers were investigated using the conventional device configuration of ITO/PEDOT:PSS/polymer blend/Al with [6,6]-phenyl C_{61}-butyric acid methyl ester ($PC_{61}BM$) as acceptor in the polymer blend. Fig. 5 shows the film absorption of P(BTI-F) and P(BTI-B) thin films blended with $PC_{61}BM$ at their optimized weight ratios for device operation. The optimized blend ratios for the two polymers are different as the molecular structure of the two polymers, their miscibility with $PC_{61}BM$ and the resulting film morphology are different. The best weight ratio for P(BTI-F) and $PC_{61}BM$ solar cells is 1 : 2; while for P(BTI-B) and $PC_{61}BM$ devices, the value is 1 : 1. These blended polymer films were prepared from 1,2-dichlorobenzene solution without thermal annealing and the absorption profiles are normalized with respect to the absorption maximum peak of $PC_{61}BM$ at 330 nm. It should be noted that even the profiles are normalized with lower PCBM content for P(BTI-B), the absorption intensity from P(BTI-B) in P(BTI-B):$P_{61}CBM$ composite is still stronger in the longer wavelength range than that of P(BTI-F):$PC_{61}BM$ blend film. This is very likely to generate larger electrical current under short-circuit conditions

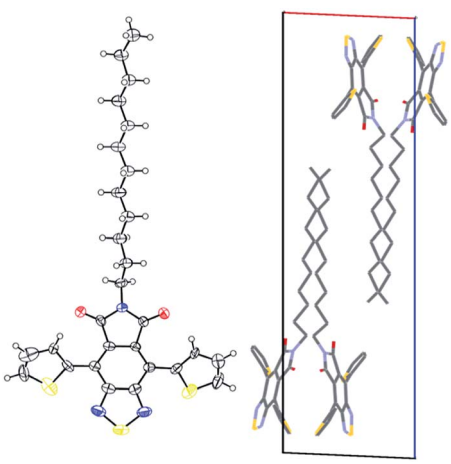

Fig. 4 Molecular geometry of compound **5** and its crystal packing viewed from axis *b*.†

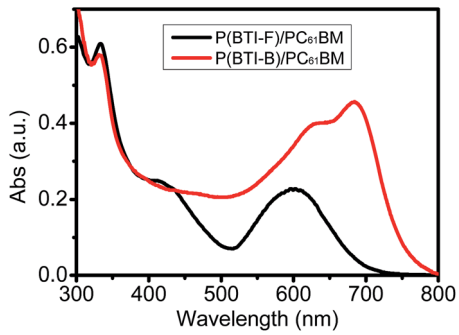

Fig. 5 Normalized UV-Vis absorbance of P(BTI-F):$PC_{61}BM$ and P(BTI-B):$PC_{61}BM$ films.

for the devices based on P(BTI-B):$PC_{61}BM$ if transport in these films is not an issue.

Fig. 6(a) shows current density–voltage (J–V) characteristics of P(BTI-F):$PC_{61}BM$ and P(BTI-B):$PC_{61}BM$ solar cells under AM 1.5G illumination (100 mW cm^{-2}). The results are summarized in Table 2. P(BTI-F):$PC_{61}BM$ device exhibits a PCE of 1.61%, with J_{sc} of 4.36 mA cm^{-2}, V_{oc} of 1.11 V, and FF of 0.33. By contrast P(BTI-B):$PC_{61}BM$ device shows a PCE of 3.42%, with J_{sc} of 9.71 mA cm^{-2}, V_{oc} of 0.75 and FF of 0.47. Hence, our P(BTI-B):$PC_{61}BM$ device is more than twice as efficient as the device based on P(BTI-F) in converting photons to electrons. The device based on P(BTI-F):$PC_{61}BM$ has a very high V_{oc} (1.11 eV) in comparison with the device based on P(BTI-B):$PC_{61}BM$. To best of our knowledge this is one of the highest V_{oc} value reporteds

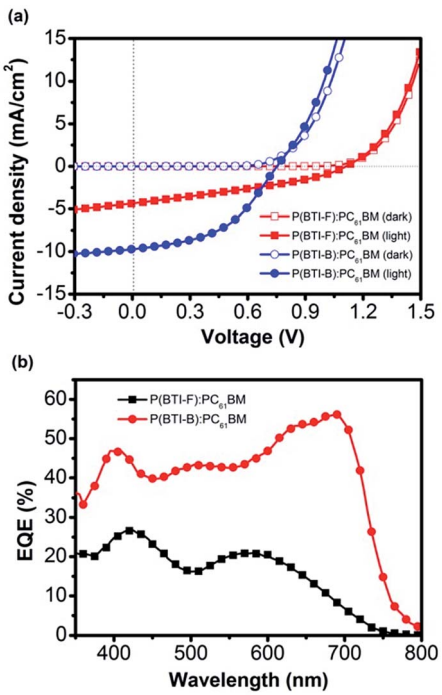

Fig. 6 (a) Current density–voltage (J–V) characteristics of P(BTI-F):$PC_{61}BM$ and P(BTI-B):$PC_{61}BM$ solar cells and (b) their corresponding external quantum efficiency (EQE) profiles.

Table 2 Photovoltaic performance of the polymers

Polymers	V_{oc} (V)	J_{sc} (mA cm^{-2})	FF	PCE (%)
P(BTI-F)	1.11	4.0	0.33	1.61
P(BTI-B)	0.75	9.8	0.47	3.42

for a single-junction cell using a polymer:fullerene blend[76–78] and this is mainly attributed to the lower lying HOMO energy level (5.59 eV) of P(BTI-F).[79] The series resistance (R_s) of the devices were also extracted from the slope of their J–V curves under light near the open circuit voltage. It was found that R_s for the P(BTI-F):$PC_{61}BM$ device was 86 Ω cm^2 and for the P(BTI-B):$PC_{61}BM$ device it was 32 Ω cm^2. Two possible reasons may contribute to a high series resistance – poor charge transport as a result of morphology or inherent mobility, and a rough interface between the polymer and electrodes. From the AFM measurements (Fig. 7), it can be seen that P(BTI-F):$PC_{61}BM$ film is smoother and has larger nano-domains. The former observation suggests that the contact between the film and Al cathode should be better and the latter observation suggests that the transport of the charges should be better. Based on the above

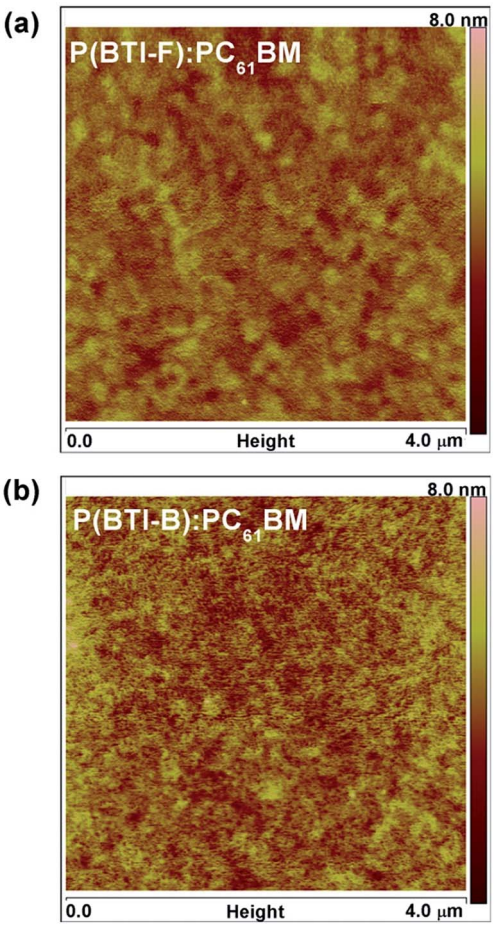

Fig. 7 AFM images of (a) P(BTI-F):$PC_{61}BM$ and (b) P(BTI-B):$PC_{61}BM$ blend films.

discussion, series resistance of P(BTI-F):$PC_{61}BM$ device ought to be lower but this is not the case and therefore, the mobility of charge carriers in P(BTI-F):$PC_{61}BM$ film must be poorer compared to P(BTI-B):$PC_{61}BM$ film. The higher charge mobility together with the higher absorption of polymer P(BTI-B) result in the higher J_{sc} seen in P(BTI-B):$PC_{61}BM$ device. The FF of both devices are only around 40%, which may indicate that the charge transport of electrons and holes is not balanced in these organic solar cells.[80] It is worth mentioning that compared to our previously reported polymers based on dicarboxylic imide-substituted isothianaphthene units, the performance of solar cells based on the structurally similar dicarboxylic imide-substituted benzothiadizole unit in this work has been significantly improved due to the stronger acceptor nature of the latter unit.[66]

Recently Wang *et al.* have also reported two low bandgap polymers with the same BDT-T-BTI backbone as in our polymer P(BTI-B), and that solar cells based on these two polymers also showed efficient performance.[68] This agrees with our finding that the combination of dicarboxylic imide-substituted benzothiadiazole (BTI) unit and benzodithiophene (BDT) units can be an effective D–A system to construct low bandgap polymers for efficient polymer solar cells. It can be seen from comparing their results with ours, that the photophysical properties of polymers based on BTI–BDT is very sensitive to the side chains attached to the main chain, so that the device performance can vary considerably depending on the number, type and size of side chains employed. For instance, when linear alky chains are adopted both for the BTI and BDT units in P(BTI-B), the polymer has a HOMO level of 5.44 eV; but a polymer with branched alkyl chains on both BTI and BDT units reported by Wang, has a HOMO level of 5.36 eV.[68] This shows linear alkyl chains can induce a deeper lying HOMO level (*ca.* 80 meV shift) than branched alkyl chains, which may result from stronger intermolecular interactions between the main chains. One interesting observation is that solar cells based on the conjugated polymer with linear alkyl chains showed a J_{sc} which is more than 1.5 times higher than that of the polymer with branched alkyl chains (9.8 mA cm^{-2} *vs.* 5.5 mA cm^{-2}) with similar V_{oc} and FF values, even though an inferior electron acceptor was used ($PC_{61}BM$ *vs.* $PC_{71}BM$). This implies that the polymer with linear alkyl chains also possesses higher hole mobility, which can be attributed to better π–π stacking of the polymer chains. On the other hand, Wang *et al.* have shown that a BTI–BDT polymer with conjugated thienyl side groups on the BDT unit has a deeper lying HOMO energy level and much higher carrier mobility than that with branched alkyl chains.[68] All these comparisons imply that for this BTI–BDT system, more planarity and better π–π stacking are desired for better charge transportation.

The external quantum efficiency (EQE) profiles of the devices are shown in Fig. 6(b). It can be seen that photovoltaic cells based on P(BTI-B):$PC_{61}BM$ have much better EQEs than devices based on P(BTI-F):$PC_{61}BM$, especially between 625 nm and 750 nm. This is because that polymer P(BTI-B) absorbed more strongly in this wavelength region. As expected, the J_{sc} of devices based on P(BTI-B):$PC_{61}BM$ is higher. The integrated J_{sc} calculated from EQE of P(BTI-F):$PC_{61}BM$ device and P(BTI-B):$PC_{61}BM$ device are 4.0 mA cm^{-2} and 9.8 mA cm^{-2} respectively, which agrees well with the measured J_{sc}.

AFM was used to study the nano-morphology of the active layers of the polymer devices, which have a strong impact on their corresponding photovoltaic properties. From the topographical AFM image shown in Fig. 6, it can be found that both films have well-distributed nano-sized domains with small film roughness. The root-mean-square (RMS) roughness (R_q) of P(BTI-F):$PC_{61}BM$ film and P(BTI-B):$PC_{61}BM$ are 0.57 nm and 0.84 nm, respectively. This shows that both polymers are reasonably miscible with $PC_{61}BM$. While P(BTI-F):$PC_{61}BM$ film has larger domains; the films based on P(BTI-B):$PC_{61}BM$ has finer domains but the roughness is higher. The larger phase separation in the blend film of P(BTI-F):$PC_{61}BM$ can be linked to the bulky fluorene unit in P(BTI-F), which further highlights the role of side chains in determining the intermolecular interaction and the blend morphology thereof. These finer domains in P(BTI-B):$PC_{61}BM$ are beneficial for the exciton separation and the rougher film does not seem to impact the series resistance negatively. As a result, the devices based on P(BTI-B):$PC_{61}BM$ showed higher short-circuit current (J_{sc}) and fill factor (FF) and hence showed higher measured efficiency compared to P(BTI-F):$PC_{61}BM$ devices.

From the model developed by Scharber *et al.*[79] one can predict maximum PCEs for these polymers with $PC_{61}BM$ of above 7% based on their bandgaps and LUMO levels. Our device results were well below this for various reasons. Firstly, we have yet to determine what aliphatic chains will give the best chain packing so as to optimise the photophysical and morphological properties, though given the superior performance of our P(BTI-B) to a similar polymer with branched chains we can already conclude that straight chains are better than branched ones; secondly, we used a standard device fabrication technique without further optimization steps such as adopting blocking/injection layers, additives, or using $PC_{71}BM$, *etc.* We anticipate that use of any or all of these would lead to marked improvements in device efficiencies, especially for P(BTI-F).

Conclusions

We report an improved synthesis of pyrrolo[3,4-*f*]-2,1,3-benzothiadiazole-5,7-dione (BTI) and the synthesis and characterization of two new D–A polymers using BTI as the electron acceptor. These polymers showed high thermal stability, excellent solubility and reduced band gaps. Our preliminary photovoltaic measurements indicated these polymers have considerable potential: P(BTI-F) had a deep lying HOMO level of −5.6 eV which directly led to an exceptionally large V_{oc} of 1.1 V, though the overall device performance (PCE 1.61%) was mediocre due to poor charge carrier mobility. Replacing the weak donor fluorene with dialkoxybenzodithiophene significantly increased the J_{sc}, FF and PCE (3.42%) but markedly reduced the V_{oc} to 0.77 V. The efficiency of the latter materials was superior to that of a similar copolymer reported elsewhere with branched instead of linear alkyl substituents suggesting that linear alkyl chains promote higher device efficiencies, probably through

better chain packing. While there remains considerable scope for further optimisation of the polymeric structures and OPV devices to fully explore the potential of BTI based polymers in photovoltaic applications, such as choosing more suitable donors in the polymer design to balance the J_{sc} and V_{oc}, inserting suitable charge injection/blocking layer to improve FF and replacing $PC_{61}BM$ with $PC_{71}BM$, or using additives, these results in combination with the easier access to the materials due to our new synthesis, suggest BTI-based copolymers are attractive candidates for the development of high performance OPVs.

Notes and references

1 P. Ding, C.-C. Chu, Y. Zou, D. Xiao, C. Pan and C.-S. Hsu, *J. Appl. Polym. Sci.*, 2012, **123**, 99–107.
2 H. Zhou, L. Yang, A. C. Stuart, S. C. Price, S. Liu and W. You, *Angew. Chem., Int. Ed. Engl.*, 2011, **50**, 2995–2998.
3 H. Yi, S. Al-Faifi, A. Iraqi, D. C. Watters, J. Kingsley and D. G. Lidzey, *J. Mater. Chem.*, 2011, **21**, 13649–13656.
4 Y. Yuan, T. J. Reece, P. Sharma, S. Poddar, S. Ducharme, A. Gruverman, Y. Yang and J. Huang, *Nat. Mater.*, 2011, **10**, 296–302.
5 L.-Y. Lin, Y.-H. Chen, Z.-Y. Huang, H.-W. Lin, S.-H. Chou, F. Lin, C.-W. Chen, Y.-H. Liu and K.-T. Wong, *J. Am. Chem. Soc.*, 2011, **133**, 15822–15825.
6 Z. B. Lim, B. Xue, S. Bomma, H. Li, S. Sun, Y. M. Lam, W. J. Belcher, P. C. Dastoor and A. C. Grimsdale, *J. Polym. Sci., Part A: Polym. Chem.*, 2011, **49**, 4387–4397.
7 U. R. Lee, T. W. Lee, M. H. Hoang, N. S. Kang, J. W. Yu, K. H. Kim, K.-G. Lim, T.-W. Lee, J.-I. Jin and D. H. Choi, *Org. Electron.*, 2011, **12**, 269–278.
8 J. E. Donaghey, R. S. Ashraf, Y. Kim, Z. G. Huang, C. B. Nielsen, W. Zhang, B. Schroeder, C. R. G. Grenier, C. T. Brown, P. D'Angelo, J. Smith, S. Watkins, K. Song, T. D. Anthopoulos, J. R. Durrant, C. K. Williams and I. McCulloch, *J. Mater. Chem.*, 2011, **21**, 18744–18752.
9 S. Ellinger, K. R. Graham, P. Shi, R. T. Farley, T. T. Steckler, R. N. Brookins, P. Taranekar, J. Mei, L. A. Padilha, T. R. Ensley, H. Hu, S. Webster, D. J. Hagan, E. W. Van Stryland, K. S. Schanze and J. R. Reynolds, *Chem. Mater.*, 2011, **23**, 3805–3817.
10 C. Du, C. Li, W. Li, X. Chen, Z. Bo, C. Veit, Z. Ma, U. Wuerfel, H. Zhu, W. Hu and F. Zhang, *Macromolecules*, 2011, **44**, 7617–7624.
11 S. Cho, J. Lee, M. Tong, J. H. Seo and C. Yang, *Adv. Funct. Mater.*, 2011, **21**, 1910–1916.
12 D.-G. Chen, Y. Yang, C. Zhong, Z.-R. Yi, F. Wu, L. Qu, Y. Li, Y.-F. Li and J.-U. Qin, *J. Polym. Sci., Part A: Polym. Chem.*, 2011, **49**, 3852–3862.
13 S. Chen, Q. Zhang, Q. Liu, J. Gu, L. Zhang, J. Zhou, X. Fan and L. Fang, *React. Funct. Polym.*, 2011, **71**, 1008–1015.
14 J. T. Bloking, X. Han, A. T. Higgs, J. P. Kastrop, L. Pandey, J. E. Norton, C. Risko, C. E. Chen, J.-L. Brédas, M. D. McGehee and A. Sellinger, *Chem. Mater.*, 2011, **23**, 5484–5490.
15 W. Cai, M. Wang, J. Zhang, E. Wang, T. Yang, C. He, J. S. Moon, H. Wu, X. Gong and Y. Cao, *J. Phys. Chem. C*, 2011, **115**, 2314–2319.
16 D. Baran, G. Oktem, S. Celebi and L. Toppare, *Macromol. Chem. Phys.*, 2011, **212**, 799–805.
17 T. W. Lee, N. S. Kang, J. W. Yu, M. H. Hoang, K. H. Kim, J.-I. Jin and D. H. Choi, *J. Polym. Sci., Part A: Polym. Chem.*, 2010, **48**, 5921–5929.
18 S. Steinberger, A. Mishra, E. Reinold, C. M. Müller, C. Uhrich, M. Pfeiffer and P. Bäuerle, *Org. Lett.*, 2010, **13**, 90–93.
19 M. Sendur, A. Balan, D. Baran, B. Karabay and L. Toppare, *Org. Electron.*, 2010, **11**, 1877–1885.
20 G. Y. Chen, S. C. Lan, P. Y. Lin, C. W. Chu and K. H. Wei, *J. Polym. Sci., Part A: Polym. Chem.*, 2010, **48**, 4456–4464.
21 T. Cai, Y. Zhou, E. Wang, S. Hellström, F. Zhang, S. Xu, O. Inganäs and M. R. Andersson, *Sol. Energy Mater. Sol. Cells*, 2010, **94**, 1275–1281.
22 H. Zhou, L. Yang, S. Xiao, S. Liu and W. You, *Macromolecules*, 2009, **43**, 811–820.
23 J. M. Winfield, A. Van Vooren, M.-J. Park, D.-H. Hwang, J. Cornil, J.-S. Kim and R. H. Friend, *J. Chem. Phys.*, 2009, **131**, 035104–035105.
24 S. Wen, J. Pei, Y. Zhou, P. Li, L. Xue, Y. Li, B. Xu and W. Tian, *Macromolecules*, 2009, **42**, 4977–4984.
25 E. Wang, M. Wang, L. Wang, C. Duan, J. Zhang, W. Cai, C. He, H. Wu and Y. Cao, *Macromolecules*, 2009, **42**, 4410–4415.
26 S. P. Mishra, A. K. Palai, R. Srivastava, M. N. Kamalasanan and M. Patri, *J. Polym. Sci., Part A: Polym. Chem.*, 2009, **47**, 6514–6525.
27 J.-J. Kim, H. Choi, J.-W. Lee, M.-S. Kang, K. Song, S. O. Kang and J. Ko, *J. Mater. Chem.*, 2008, **18**, 5223–5229.
28 J. Hou, M.-H. Park, S. Zhang, Y. Yao, L.-M. Chen, J.-H. Li and Y. Yang, *Macromolecules*, 2008, **41**, 6012–6018.
29 J. Hou, H.-Y. Chen, S. Zhang, G. Li and Y. Yang, *J. Am. Chem. Soc.*, 2008, **130**, 16144–16145.
30 C. Soci, I.-W. Hwang, D. Moses, Z. Zhu, D. Waller, R. Gaudiana, C. J. Brabec and A. J. Heeger, *Adv. Funct. Mater.*, 2007, **17**, 632–636.
31 J. Roncali, *Macromol. Rapid Commun.*, 2007, **28**, 1761–1775.
32 C.-H. Chen, J. T. Lin and M.-C. P. Yeh, *Org. Lett.*, 2006, **8**, 2233–2236.
33 A. J. A. B. Seeley, R. H. Friend, J.-S. Kim and J. H. Burroughes, *J. Appl. Phys.*, 2004, **96**, 7643–7649.
34 Y. Kim, S. Cook, S. A. Choulis, J. Nelson, J. R. Durrant and D. D. C. Bradley, *Chem. Mater.*, 2004, **16**, 4812–4818.
35 J. D. Yuen, R. Kumar, D. Zakhidov, J. Seifter, B. Lim, A. J. Heeger and F. Wudl, *Adv. Mater.*, 2011, **23**, 3780–3785.
36 K. Ono, S. Tanaka and Y. Yamashita, *Angew. Chem., Int. Ed. Engl.*, 1994, **33**, 1977–1979.
37 T. Kono, D. Kumaki, J.-I. Nishida, S. Tokito and Y. Yamashita, *Chem. Commun.*, 2010, **46**, 3265–3267.
38 G. Qian, B. Dai, M. Luo, D. Yu, J. Zhan, Z. Zhang, D. Ma and Z. Y. Wang, *Chem. Mater.*, 2008, **20**, 6208–6216.
39 M. Karikomi, C. Kitamura, S. Tanaka and Y. Yamashita, *J. Am. Chem. Soc.*, 1995, **117**, 6791–6792.

40 M. Wang, X. Hu, P. Liu, W. Li, X. Gong, F. Huang and Y. Cao, *J. Am. Chem. Soc.*, 2011, **133**, 9638–9641.
41 J. A. Mikroyannidis, D. V. Tsagkournos, S. S. Sharma, Y. K. Vijay and G. D. Sharma, *J. Mater. Chem.*, 2011, **21**, 4679–4688.
42 A. Thomas, K. Bhanuprakash and K. M. M. K. Prasad, *J. Phys. Org. Chem.*, 2011, **24**, 821–832.
43 X. Li, A. Liu, S. Xun, W. Qiao, X. Wan and Z. Y. Wang, *Org. Lett.*, 2008, **10**, 3785–3787.
44 T. L. Tam, H. Li, F. Wei, K. J. Tan, C. Kloc, Y. M. Lam, S. G. Mhaisalkar and A. C. Grimsdale, *Org. Lett.*, 2010, **12**, 3340–3343.
45 Y. Fu, W. Shen and M. Li, *Polym. Int.*, 2011, **60**, 211–221.
46 Y. Yamashita, K. Ono, M. Tomura and S. Tanaka, *Tetrahedron*, 1997, **53**, 10169–10178.
47 X. Wang, E. Perzon, F. Oswald, F. Langa, S. Admassie, M. R. Andersson and O. Inganas, *Adv. Funct. Mater.*, 2005, **15**, 1665–1670.
48 E. Perzon, F. Zhang, M. Andersson, W. Mammo, O. Inganäs and M. R. Andersson, *Adv. Mater.*, 2007, **19**, 3308–3311.
49 C. Kitamura, S. Tanaka and Y. Yamashita, *Chem. Lett.*, 1996, **25**, 63–64.
50 C.-Y. Yu, C.-P. Chen, S.-H. Chan, G.-W. Hwang and C. Ting, *Chem. Mater.*, 2009, **21**, 3262–3269.
51 X. Zhang, T. T. Steckler, R. R. Dasari, S. Ohira, W. J. Potscavage Jr, S. P. Tiwari, S. Coppee, S. Ellinger, S. Barlow, J.-L. Bredas, B. Kippelen, J. R. Reynolds and S. R. Marder, *J. Mater. Chem.*, 2010, **20**, 123–134.
52 K.-F. Cheng, C.-C. Chueh, C.-H. Lin and W.-C. Chen, *J. Polym. Sci., Part A: Polym. Chem.*, 2008, **46**, 6305–6316.
53 H. Yi, R. G. Johnson, A. Iraqi, D. Mohamad, R. Royce and D. G. Lidzey, *Macromol. Rapid Commun.*, 2008, **29**, 1804–1809.
54 Y. Lee, T. P. Russell and W. H. Jo, *Org. Electron.*, 2010, **11**, 846–853.
55 T. Dallos, M. Hamburger and M. Baumgarten, *Org. Lett.*, 2011, **13**, 1936–1939.
56 A. P. Zoombelt, M. Fonrodona, M. M. Wienk, A. B. Sieval, J. C. Hummelen and R. A. J. Janssen, *Org. Lett.*, 2009, **11**, 903–906.
57 E. Perzon, X. Wang, S. Admassie, O. Inganäs and M. R. Andersson, *Polymer*, 2006, **47**, 4261–4268.
58 G. Zhang, Y. Fu, Q. Zhang and Z. Xie, *Polymer*, 2010, **51**, 2313–2319.
59 O. Inganäs, F. Zhang, K. Tvingstedt, L. M. Andersson, S. Hellstrom and M. R. Andersson, *Adv. Mater.*, 2010, **22**, E100–E116.
60 M. Luo, H. Shadnia, G. Qian, X. Du, D. Yu, D. Ma, J. S. Wright and Z. Y. Wang, *Chem.–Eur. J.*, 2009, **15**, 8902–8908.
61 C. Kitamura, S. Tanaka and Y. Yamashita, *Chem. Mater.*, 1996, **8**, 570–578.
62 E. K. Unver, S. Tarkuc, D. Baran, C. Tanyeli and L. Toppare, *Tetrahedron Lett.*, 2011, **52**, 2725–2729.
63 H. Li, F. Zhou, T. L. D. Tam, Y. M. Lam, S. G. Mhaisalkar, H. Su and A. C. Grimsdale, *J. Mater. Chem. C*, 2013, **1**, 1745–1752.
64 C. M. Cardona, W. Li, A. E. Kaifer, D. Stockdale and G. C. Bazan, *Adv. Mater.*, 2011, **23**, 2367–2371.
65 Y.-Q. Feng, D.-X. Shi, H.-L. Chen, L.-S. Zhou and B. Zhang, *J. Tianjin Univ.*, 2002, **35**, 652–654.
66 H. Li, S. Sun, T. Salim, S. Bomma, A. C. Grimsdale and Y. M. Lam, *J. Polym. Sci., Part A: Polym. Chem.*, 2012, **50**, 250–260.
67 H. Li, T. M. Koh, A. Hagfeldt, M. Gratzel, S. G. Mhaisalkar and A. C. Grimsdale, *Chem. Commun.*, 2013, **49**, 2409–2411.
68 L. Wang, D. Cai, Q. Zheng, C. Tang, S.-C. Chen and Z. Yin, *ACS Macro Lett.*, 2013, **2**, 605–608.
69 J. Shao, J. Chang and C. Chi, *Org. Biomol. Chem.*, 2012, **10**, 7045–7052.
70 P.-T. Wu, F. S. Kim, R. D. Champion and S. A. Jenekhe, *Macromolecules*, 2008, **41**, 7021–7028.
71 Y. Zou, A. Najari, P. Berrouard, S. Beaupré, B. Réda Aïch, Y. Tao and M. Leclerc, *J. Am. Chem. Soc.*, 2010, **132**, 5330–5331.
72 L. Huo, J. Hou, S. Zhang, H.-Y. Chen and Y. Yang, *Angew. Chem., Int. Ed. Engl.*, 2010, **49**, 1500–1503.
73 Y. Liang, Z. Xu, J. Xia, S.-T. Tsai, Y. Wu, G. Li, C. Ray and L. Yu, *Adv. Mater.*, 2010, **22**, E135–E138.
74 H.-Y. Chen, J. Hou, S. Zhang, Y. Liang, G. Yang, Y. Yang, L. Yu, Y. Wu and G. Li, *Nat. Photonics*, 2009, **3**, 649–653.
75 J. Hou, H.-Y. Chen, S. Zhang, R. I. Chen, Y. Yang, Y. Wu and G. Li, *J. Am. Chem. Soc.*, 2009, **131**, 15586–15587.
76 J. C. Bijleveld, R. A. M. Verstrijden, M. M. Wienk and R. A. J. Janssen, *Appl. Phys. Lett.*, 2010, **97**, 073304.
77 C. Guo, Y.-H. Lin, M. D. Witman, K. A. Smith, C. Wang, A. Hexemer, J. Strzalka, E. D. Gomez and R. Verduzco, *Nano Lett.*, 2013, **13**, 2957–2963.
78 C. R. McNeill, A. Abrusci, J. Zaumseil, R. Wilson, M. J. McKiernan, J. H. Burroughes, J. J. M. Halls, N. C. Greenham and R. H. Friend, *Appl. Phys. Lett.*, 2007, **90**, 193506.
79 M. C. Scharber, D. Mühlbacher, M. Koppe, P. Denk, C. Waldauf, A. J. Heeger and C. J. Brabec, *Adv. Mater.*, 2006, **18**, 789–794.
80 P. Sonar, E. L. Williams, S. P. Singh and A. Dodabalapur, *J. Mater. Chem.*, 2011, **21**, 10532–10541.